PCCP

Ball-Milled Sulfur-Doped Graphene Materials Contain Metallic Impurities Originating from Ball-Milling Apparatus: Influence on the Catalytic Properties

Journal:	*Physical Chemistry Chemical Physics*
Manuscript ID	CP-ART-05-2016-003004.R1
Article Type:	Paper
Date Submitted by the Author:	28-May-2016

Complete List of Authors:	Chua, Chun Kiang; Nanyang Technological University, Chemistry and Biological Chemistry Sofer, Zdenek; Institute of Chemical Technology, Prague, Department of Inorganic Chemistry Khezri, Bahareh; Nanyang Technological University, School of Physical and Mathematical Sciences Webster, Richard; Nanyang Technological University, Division of Chemistry and Biological Chemistry Pumera, Martin; Nanyang Technological University, Chemistry and Biological Chemistry

Journal Name

ARTICLE

Ball-Milled Sulfur-Doped Graphene Materials Contain Metallic Impurities Originating from Ball-Milling Apparatus: Influence on the Catalytic Properties

Received 00th January 20xx,
Accepted 00th January 20xx

DOI: 10.1039/x0xx00000x

www.rsc.org/

Chun Kiang Chua,[a] Zdeněk Sofer,[b] Bahareh Khezri,[a] Richard D. Webster,[a] Martin Pumera*[a]

Graphene materials have found applications in a wide range of devices over the past decade. In order to meet the demand for graphene materials, various synthesis methods are constantly being improved or invented. Ball-milling of graphite to obtain graphene materials is one of the many versatile methods to easily obtain bulk quantity. In this work, we show that the graphene materials produced by ball-milling are spontaneously contaminated with metallic impurities originating from the grinding bowls and balls. Ball-milled sulfur-doped graphene materials obtained from two types of ball-milling apparatus, specifically made up of stainless steel and zirconium dioxide, were investigated. Zirconium dioxide-based ball-milled sulfur-doped graphene material contains drastically lower amount of metallic impurities than stainless steel-based ball-milled sulfur-doped graphene material. The presence of metallic impurities is demonstrated by their catalytic effects toward the electrochemical catalysis of hydrazine and cumene hydroperoxide. The general impression toward ball-milling of graphite as a versatile method for bulk production of 'metal-free' graphene materials without the need for post-processing and the selection of ball-milling tools should be cautioned. These findings would have wide-reaching implications to graphene research.

Introduction

After more than a decade of research on graphene since it was first isolated in 2004, its exceptional physical, mechanical and chemical features[1, 2] have greatly improved the performance of modern devices in research areas ranging from electronic,[3, 4] photonic,[5] energy storage and production,[6, 7] healthcare,[8] electrochemical sensing[9] to composite materials[10]. These promising applications have spurred research on more effective and economical synthesis methods to produce high-quality pristine graphene (a single layer "polycyclic aromatic hydrocarbon of quasi infinite size" without structural defects in its carbon sp^2 plane)[11]. Although the bulk production of high-quality pristine graphene has yet to be realized, several methods have been developed to obtain near-pristine graphene.[9, 12, 13] These methods can be categorized into two major strategies, mainly bottom-up and top-down methods. The bottom-up method aims to produce graphene from small molecular building blocks (e.g. chemical vapour deposition, epitaxial growth, chemical synthesis) while the top-down method relies on the exfoliation of graphite (e.g. chemical, thermal, electrochemical, solution-based and mechanical exfoliation). To date, the top-down approach has proven to be more economical, at the expense of quality. Furthermore, it is interesting to note that the mechanical exfoliation of graphite by dry ball-milling has not been widely studied.

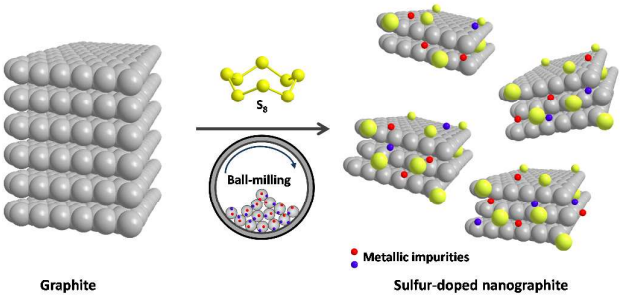

Figure 1. Schematic for the preparation of sulfur-doped nanographite. Graphite is ball-milled in the presence of sulfur with grinding bowls and balls made up of stainless steel and zirconium oxide. The metallic contents of the grinding bowls and balls are transferred to the produced nanographite materials during ball-milling process.

Ball-milling is a common technique in the powder production industry to acquire grains of specific dimensions. This is performed by placing solid materials of interest in a grinding bowl filled with grinding balls and subsequent rotational motion of the grinding bowl causes the grinding balls to impact onto the solid materials repeatedly over a stipulated time period. In the case of graphite, exfoliation and

[a] Division of Chemistry and Biological Chemistry, School of Physical and Mathematical Sciences, Nanyang Technological University, Singapore 637371, Singapore.
[b] Institute of Chemical Technology, Department of Inorganic Chemistry, 16628 Prague 6, Czech Republic.
Email: pumera@ntu.edu.sg
Electronic Supplementary Information (ESI) available: EDS, elemental analysis, survey XPS data and supporting cyclic voltammetry analyses. See
DOI: 10.1039/x0xx00000x

fragmentation effects are readily achieved from the respective shear and collision forces exerted by the balls during dry ball milling process.[14] Although the extent of defects induced by the milling process is not as clear, acidic group-functionalized graphene has been obtained by milling graphite in the presence of carbon dioxide, sulfur trioxide or carbon dioxide/sulfur trioxide mixture.[15, 16] In other cases, hydrogen, halogens and sulfur elements were embedded onto graphene sheets *via* ball-milling.[17, 18] Furthermore, sulfur-doped graphene has been applied for lithium-sulfur batteries[19] and as electrocatalyst for the oxygen reduction reaction[18]. More recently, the doping of semi-metal antimony onto the edges of graphene nanoplatelets *via* ball-milling technique has been achieved.[20]

As the grinding bowl and balls can be composed of a wide range of materials (i.e. stainless steel, tempered steel, zirconium oxide, silicon nitride, sintered corundum, tungsten carbide, agate), various qualities of fabricated ball-milled graphene materials can be derived. We are especially concern about the introduction of metallic impurities onto the ball-milled graphene materials as a result of varying the types of grinding bowl and balls. This problem is further aggravated by the lack of post-processing purifications. While the influences of metallic impurities on the electronic,[21, 22] redox,[23, 24] electrochemical,[25-28] adsorption[29] and toxicological[30, 31] properties in carbon nanotubes have already been widely acknowledged, research on the effects of metallic impurities on graphene and graphene related materials are still picking up.[9] Metallic impurities in graphene have been identified to be responsible for their electrocatalytic[32-34] properties. On that note, our group has previously identified that the metallic impurities in chemically produced graphene could originate from the source of graphite[35] and chemical reagents[34-37] applied during synthesis. In addition, such metallic contamination issue is also highly prevalent in CVD graphene with no immediate solutions.[38-40] The content of metallic impurities from ball-milled graphene materials has, however, not been investigated.

In this work, we investigate the content of metallic impurities in sulfur-doped nanographite prepared *via* ball-milling technique (**Figure 1**). We evaluate two types of ball-milled nanographite fabricated from their respective set of grinding bowl and balls made up of stainless steel (316L) and zirconium dioxide. We show that the type of materials employed as grinding bowls and balls can produce nanographite with large disparities in their metallic contents. The catalytic abilities of these two types of ball-milled sulfur-doped nanographite, due to the presence of metallic impurities, are demonstrated with the electro-oxidation of hydrazine and electro-reduction of cumene hydroperoxide.

Experimental Section

Materials

Graphite (2-15 μm, 99.9995 %) was obtained from Alfa Aesar, Germany. Sulfur (99.999 %) was obtained from STREM, Germany. Carbon disulfide and isopropanol were obtained from Penta, Czech Republic. Argon (purity 99.996 %) was obtained from SIAD, Czech Republic. Cumene hydroperoxide (80 %), hydrazine monohydrate (98 %), chromium(VI) oxide and manganese(IV) oxide powder were purchased from Alfa Aesar, Singapore. Copper nanopowder, copper(I) oxide powder, copper(II) oxide nanopowder, molybdenum nanopowder, molybdenum(IV) oxide powder, molybdenum(VI) oxide powder, iron(II) oxide powder, iron(II,III) oxide nanopowder, nickel nanopowder and nickel(II) oxide nanopowder were purchased from Sigma Aldrich, Singapore. Milli-Q water (resistivity: 18.2 MΩ.cm) was used throughout the experiments.

Apparatus

X-ray photoelectron spectroscopy was performed with Phoibos 100 spectrometer and Mg X-ray radiation source (SPECS, Germany). Both survey and high-resolution spectra for C1s and O1s were collected. Relative sensitivity factors were used for evaluation of atomic percentage from the XPS survey spectra measurements. XPS samples were prepared by coating a carbon tape with a uniform layer of the graphene materials under study. Raman spectroscopy analysis was performed using a confocal micro-Raman LabRam HR instrument from Horiba Scientific in backscattering geometry with a CCD detector, a 514.5 nm Ar laser and a 100× objective mounted on a Olympus optical microscope. The calibration is initially made using an internal silicon reference at 520 cm^{-1} and gives a peak position resolution of less than 1 cm^{-1}. The spectra are measured from 1000 to 3000 cm^{-1}. A JEOL JSM-7600F semi-in-lens FE-SEM was used to acquire the SEM images. The graphene materials were transferred to a carbon tape held onto a SEM holder for analyses. EDX data were obtained using Oxford instrument and analysed using Aztec software. Elemental analyses were performed using an Agilent 7700 series inductively coupled plasma – mass spectrometer (ICP-MS) with a 3rd generation He reaction/collision cell to minimize interferences, and microwave digestions utilizing ultrapure concentrated nitric acid were performed on a Mars CEM system. All voltammetric experiments were performed on a μAutolab type III electrochemical analyser (Eco Chemie, The Netherlands) connected to a personal computer and controlled by General Purpose Electrochemical Systems Version 4.9 software (Eco Chemie).

Procedures

The synthesis of sulfur doped nanographite was performed by high energy ball milling using planetary micro mill Pulverisette 7 (Fritsch, Germany). Graphite (8 g) and sulfur (1 g) was placed in 45 ml grinding bowl and 70 g of milling balls was added. The grinding bowl was flushed with argon and the milling was

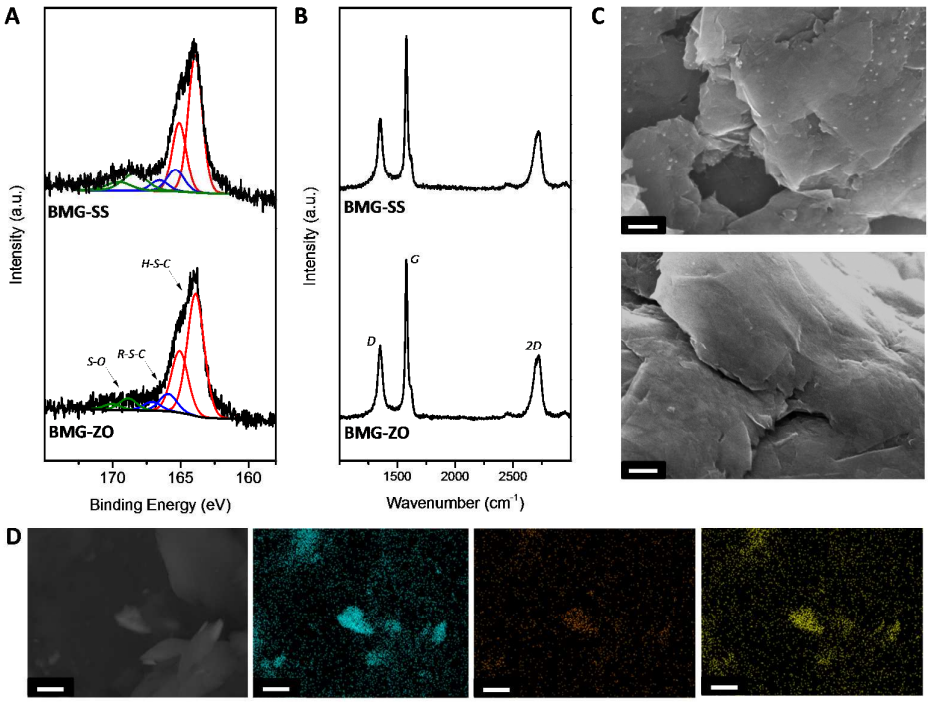

Figure 2. Structural and morphological characterisations of BMG-SS and BMG-ZO. (A) X-ray photoelectron spectra of S2p core-level scans. (B) Raman spectra. (C) SEM images of BMG-SS (top) and BMG-ZO (bottom) at 60000× magnification. Scale bar represents 200 nm. (D) EDS analysis on BMG-SS including the SEM image, iron (cyan), nickel (orange) and chromium (yellow). Scale bar represents 3 µm.

performed over 24 hr at 800 rpm. Two sets of milling apparatus were utilized, whereby a set of grinding bowl and milling balls were made up of stainless steel (316L) while the other set was made up of zirconium oxide. The sulfur-doped nanographite made by high energy ball milling was removed from grinding bowl by washing with isopropanol and separated by suction filtration. The unreacted sulfur was removed from the nanographite by Soxhlet extractor and carbon disulfide.

Electrochemical Measurements

The EPPG and GC electrode surfaces were polished 0.05 µm alumina on a polishing cloth prior to usage. Immobilization of graphene materials on the working electrodes was performed by depositing 1 µL of the desired materials (graphene materials or metal particles at 5 mg/mL dispersed in DMF with 60 min ultrasonication treatment) onto the surfaces of glassy carbon electrodes. The electrochemical experiments were carried out in a 10 mL voltammetric cell at room temperature using a three-electrode configuration. A platinum electrode served as an auxiliary electrode and a Ag/AgCl electrode as a reference electrode. Cyclic voltammetry experiments were performed at a scan rate of 100 mV s^{-1} using 50 mM phosphate buffered solution (pH 7.2) as supporting electrolyte and 10 mM CHP or 5 mM hydrazine as molecular probes. Blank measurements performed with the metallic particles in solution containing only phosphate buffered solution did not show prominent reduction/oxidation waves unless otherwise stated.

Results and discussion

Traces of metallic impurities are prevalent in all classes of carbon materials.[9] Although it is hard to prevent such contamination, the presence of metallic impurities should not be ignored since they are able to influence the electrochemical responses of the carbon materials. In order to minimize this effect, nuclear reactor-grade graphite was applied as starting material in this work for ball-milling due to its high purity.[36] As our group has always advocated thorough characterization of graphene and graphene related materials to avoid possible misrepresentation of their catalytic effects,[9, 34-37, 41] we have performed detailed detections of trace metallic impurities on the sulfur-doped nanographite materials. Both nanographite materials prepared using stainless steel (BMG-SS) and zirconium dioxide (BMG-ZO) grinding tools were subjected to trace metals analysis with inductively-coupled plasma mass spectrometry (ICP-MS). Six of the most abundant metals, in particular, Fe, Cr, Ni, Mo, Mn and Cu are shown in **Table 1**. The concentration of metals in BMG-SS drastically surpassed that of BMG-ZO. Since stainless steel of grade 316L is a standard molybdenum-bearing grade that consists predominantly of a mixture of Fe, Cr, Ni, Mo and Mn, it can be inferred from the ICP-MS results that the high content of metals could originate

Table 1. Elemental concentration of metals (ppm by mass) present in BMG-SS and BMG-ZO as determined by ICP-MS.

	Elemental concentration (ppm)					
Material	**Fe**	**Cr**	**Ni**	**Mo**	**Mn**	**Cu**
BMG-SS	81657	19907	11998	2328	1802	466
BMG-ZO	95	8	8	13	4	6

from the stainless steel 316L grinding tools. In comparison to previous ICP-OES measurement performed on the ultrapure graphite starting material,[36] low composition of metals such as Fe (<0.18 ppm), Cr (<0.4 ppm), Mn (0.14 ppm) and Cu (1.2 ppm) were detected. Despite the difference in sensitivity between ICP-MS and ICP-OES, the amount of metallic impurities introduced into BMG-ZO is generally low and also comparable to common natural graphite[35]. Zirconium was detected at 10 and 109 ppm in BMG-SS and BMG-ZO, respectively. Apart from that, energy dispersive X-ray spectroscopy (EDS) analysis on BMG-SS mapped out the presence of Fe, Ni and Cr (**Figure 2D and Figure S1, Supporting Information**), which were not observed in BMG-ZO (**Figure S2, Supporting Information**).

Several structural characterization techniques were also performed to ascertain the successful fabrication of the sulfur-doped nanographite materials. First and foremost, structural analysis with X-ray photoelectron spectroscopy (XPS) established the presence of carbon, oxygen and sulfur elements based on survey scans (**Figure S3, Supporting Information**). The extent of sulfur doping based on the XPS survey scans were ~3 at% for both BMG-SS and BMG-ZO. The XPS results resonated closely to the values of ~2 at% obtained from combustible elemental analysis (**Table S1, Supporting Information**). Moreover, the presence of sulfur was supported by EDS analyses (**Figure S1 and S2, Supporting Information**), which showed a homogeneous distribution of sulfur doping on BMG-SS and BMG-ZO. Subsequent breakdown on the specific chemical compositions of sulfur interpreted from the high-resolution XPS of the S2p core-level regions suggested that the thiol group was the major component while sulfonic group was the minor component (**Figure 2A**).

As S2p peaks are typically presented in spin-orbit doublets of $S2p_{3/2}$ and $S2p_{1/2}$ (with typical splitting magnitude of 1.18 eV), three $S2p_{3/2}$ peaks representing sulfur bonding of H-S-C (~163.5 eV), R-S-C (~164.5 eV) and S-O (~168.0 eV) were clearly observed. In fact, the largest peak arising from the presence of H-S-C bond indicated the successful doping of BMG-SS and BMG-ZO with predominantly thiol group (**Table S2, Supporting Information**). The R-S-C peak could arise from the presence of sulfur-based ring system while the S-O peak could represent sulfonic acid group formed by oxidised thiols. Further Raman analyses on BMG-SS and BMG-ZO (**Figure 2B**) indicated D/G band intensity ratios of approximately 0.5, which corresponded to sp^2 lattice size of approximately 35 nm. The presence of near symmetrical 2D band and high intensity G band indicated a successful exfoliation of graphite down to approximately to 3-5 layers of graphene,[42, 43] while the low

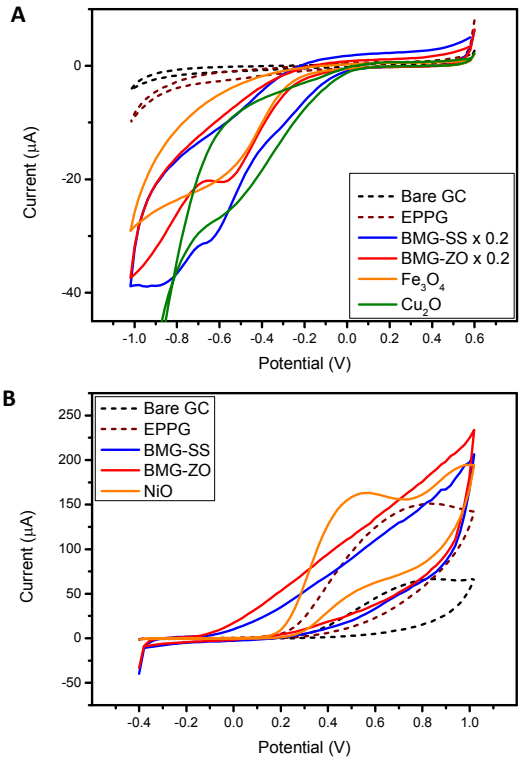

Figure 3. (A) Cyclic voltammograms for 10 mM CHP on bare GC, EPPG, BMG-SS-, BMG-ZO-, Fe_3O_4- and Cu_2O-modified electrodes. The suffix × denotes the number of times the current values of the cyclic voltammograms were scaled for ease of comparison. (B) Cyclic voltammograms for 5 mM N_2H_4 on bare GC, EPPG, BMG-SS-, BMG-ZO- and NiO-modified electrodes. Supporting electrolyte, 50 mM phosphate buffered solution at pH 7.2. Purged with N_2. Scan rate 100 mV s^{-1}. Reference electrode, Ag/AgCl.

D/G band ratios indicated low structural defects (typical chemically or thermally produced graphene had D/G bands ratio of >1)[9]. Apart from that, the scanning electron images (SEM) of BMG-SS and BMG-ZO as observed in **Figure 2C** showed stacked structures of graphene sheets.

The presence of metallic impurities in graphene materials, even at ppm levels, is known to influence their electrochemical properties.[34, 35, 44] In order to examine such possible events on BMG-SS and BMG-ZO, we investigated the effects of metallic impurities toward the reduction of cumene hydroperoxide (CHP)[35] as peroxides such as hydrogen peroxide[26] and organic peroxides[45] were previously shown to be very sensitive to reduction by Fe-based impurities. The presence of any catalytic effects would result in the lowering of the reduction potential of CHP in relative to edge-plane pyrolytic graphite (EPPG) electrode (*vide infra*). **Figure 3A** shows the representative cyclic voltammetry measurements performed in a phosphate buffer containing CHP (10 mM) with BMG-SS, BMG-ZO, bare glassy carbon (GC), EPPG, Cu_2O- and Fe_3O_4-modified electrodes. The measurements with bare GC and EPPG electrodes represented non-catalytic control cases. In the case of EPPG, since the heterogeneous electron transfer at edge plane of carbon materials is faster by a factor of 10^7 compared to basal plane,[46] any positive deviation from the performance

of EPPG can only be caused by catalytic metallic impurities. The reduction of CHP on bare GC did not show any obvious reduction peak while EPPG showed weak reduction wave at around –0.80 V. On the other hand, BMG-SS and BMG-ZO showed prominent catalytic reduction peaks at –0.65 and –0.58 V, respectively. On the other hand, the catalytic reduction peaks originating from Fe_3O_4- and Cu_2O-modified electrodes were observed at approximately –0.55 V. The close proximity and overlapping of the peaks to that of BMG-SS and BMG-ZO suggested possible catalytic effect granted by the presence of Fe- and Cu-based metallic impurities present in BMG-SS and BMG-ZO. The lower onset potential of the reduction wave of BMG-SS, as compared to BMG-ZO, was most likely due to the high content of Cu-based metallic impurities in the former. It was previously established that only a low amount of metallic catalyst was required to result in electrocatalysis.[44] Furthermore, low reduction peak potentials and low onset potentials of reduction waves observed on FeO, MoO_2 and MoO_3 also indicated positive catalytic properties toward the reduction of CHP (**Figure S4, Supporting Information**). However, no catalytic effects were observed on Mo-, Cu-, CuO-, Mo-, CrO_3-, MnO_2-, Ni- and NiO-modified electrodes (**Figure S5, Supporting Information**).

The electrocatalytic effects of BMG-SS and BMG-ZO toward the oxidation of hydrazine was subsequently examined. Ni-based nanoparticles are known to catalyse the oxidation of hydrazine by lowering the oxidation potential.[25] **Figure 3B** shows the representative cyclic voltammetry measurements performed in a phosphate buffered solution of hydrazine (5 mM) with BMG-SS, BMG-ZO, bare GC, EPPG and NiO-modified electrode. The oxidation of hydrazine on both bare GC and EPPG electrodes were observed at similar potentials (+0.80 V). On the other hand, BMG-SS and BMG-ZO showed gradual and broad oxidation slopes which began at –0.10 V. The early onset of oxidation slopes from BMG-SS and BMG-ZO coincided with that of NiO-modified electrode, which showed an oxidation wave beginning at +0.10 V with a peak at +0.55 V. This showed that NiO was likely to influence the early onset oxidation waves of both BMG-SS and BMG-ZO. Further investigations performed with Mo-, MoO_2-, MoO_3-, Cu-, CuO-, Cu_2O-, CrO_3-, MnO_2-, Fe_3O_4- and Ni-modified electrodes did not indicate any possible electrocatalytic effects (**Figure S6, Supporting Information**).

The results discussed above highlighted the unavoidable metal contamination of graphene materials that are produced by ball-milling technique. Ball-milling apparatus made up of stainless steel can introduce unprecedented amount of metallic impurities, especially Fe-based impurities, into the final graphene material. Unfortunately, most literatures on ball-milled graphene materials which applied stainless-steel apparatus fell short on accounting for the presence of trace metallic contents. Despite the application of seemingly 'metal-free' zirconium dioxide ball-milling apparatus, a small fraction of metallic impurities is still present in the resulted graphene materials. The presence of such metallic impurities is not only able to influence the electrochemical properties of the graphene materials as aforementioned, but may affect their potential usage in other applications (e.g., batteries, fuel cells, water membrane etc.). In this case, it is best to adhere to using zirconium dioxide ball-milling apparatus since the resultant graphene materials would contain a lower amount of metallic impurities. This would improve the ease of purification since common removal processes (e.g., thermal treatment at 1000 °C in Cl_2 atmosphere,[34, 47] washing with strong acids like HCl,[48] HNO_3[49-51]) could be challenging yet ineffective at times. All these are apart from the fact that the ball-milling technique also introduces structural defects to the graphene materials. Furthermore, we also underline the usage of exceedingly pure graphite as the starting material for ball-milling in this work to ensure the minimal presence of inherent metallic impurities. In actual fact, natural or synthetic graphite, which is the more economical choice of starting material, contains far higher levels of inherent metallic impurities that can further aggravate the issues discussed herein.

Conclusions

We have demonstrated that graphene materials produced by ball-milling technique were contaminated with metallic impurities originating from the grinding bowl and balls. Graphene materials produced using stainless steel apparatus contained drastically more metallic impurities than those produced using zirconium dioxide apparatus. These metallic impurities are highly active catalysts that are capable of catalysing electrochemical processes, as we have demonstrated with hydrazine and cumene hydroperoxide. Moreover, these metallic impurities may alter the electronic, redox and toxicological properties of the graphene materials. Since ball-milling of graphite is an important avenue for the mass fabrication of graphene materials, the presence of metallic impurities should be cautioned and accounted for prior to their subsequent implementation into functional devices. Our findings would have important and wide implications to graphene research in general.

Acknowledgements

M.P. acknowledges Tier 2 grant (MOE2013-T2-1-056; ARC 35/13) from the Ministry of Education, Singapore.

References

1. A. K. Geim and K. S. Novoselov, *Nat. Mater.*, 2007, **6**, 183-191.
2. K. S. Novoselov, V. I. Fal'ko, L. Colombo, P. R. Gellert, M. G. Schwab and K. Kim, *Nature*, 2012, **490**, 192-200.
3. N. O. Weiss, H. L. Zhou, L. Liao, Y. Liu, S. Jiang, Y. Huang and X. F. Duan, *Adv. Mater.*, 2012, **24**, 5782-5825.
4. J. A. Rogers, *Nat. Nanotechnol.*, 2008, **3**, 254-255.
5. F. Bonaccorso, Z. Sun, T. Hasan and A. C. Ferrari, *Nat. Photonics*, 2010, **4**, 611-622.
6. M. Pumera, *Energy Environ. Sci.*, 2011, **4**, 668-674.

7. F. Bonaccorso, L. Colombo, G. H. Yu, M. Stoller, V. Tozzini, A. C. Ferrari, R. S. Ruoff and V. Pellegrini, *Science*, 2015, **347**, 1246501.
8. K. V. Krishna, C. Menard-Moyon, S. Verma and A. Bianco, *Nanomedicine*, 2013, **8**, 1669-1688.
9. A. Ambrosi, C. K. Chua, A. Bonanni and M. Pumera, *Chem. Rev.*, 2014, **114**, 7150-7188.
10. S. Stankovich, D. A. Dikin, G. H. B. Dommett, K. M. Kohlhaas, E. J. Zimney, E. A. Stach, R. D. Piner, S. T. Nguyen and R. S. Ruoff, *Nature*, 2006, **442**, 282-286.
11. A. D. McNaught and A. Wilkinson, *Compendium of Chemical Terminology: IUPAC Recommendations*, International Union of Pure Applied Chemistry, Blackwell Science, 1997.
12. W. C. Ren and H. M. Cheng, *Nat. Nanotechnol.*, 2014, **9**, 726-730.
13. M. J. Allen, V. C. Tung and R. B. Kaner, *Chem. Rev.*, 2010, **110**, 132-145.
14. M. Yi and Z. Shen, *J. Mater. Chem. A*, 2015, **3**, 11700-11715.
15. I. Y. Jeon, H. J. Choi, S. M. Jung, J. M. Seo, M. J. Kim, L. M. Dai and J. B. Baek, *J. Am. Chem. Soc.*, 2013, **135**, 1386-1393.
16. I.-Y. Jeon, Y.-R. Shin, G.-J. Sohn, H.-J. Choi, S.-Y. Bae, J. Mahmood, S.-M. Jung, J.-M. Seo, M.-J. Kim, D. Wook Chang, L. Dai and J.-B. Baek, *Proc. Natl. Acad. Sci. U. S. A.*, 2012, **109**, 5588-5593.
17. J. T. Xu, I. Y. Jeon, J. M. Seo, S. X. Dou, L. M. Dai and J. B. Baek, *Adv. Mater.*, 2014, **26**, 7317-7323.
18. I. Y. Jeon, S. Zhang, L. P. Zhang, H. J. Choi, J. M. Seo, Z. H. Xia, L. M. Dai and J. B. Baek, *Adv. Mater.*, 2013, **25**, 6138-6145.
19. T. Q. Lin, Y. F. Tang, Y. M. Wang, H. Bi, Z. Q. Liu, F. Q. Huang, X. M. Xie and M. H. Jiang, *Energy Environ. Sci.*, 2013, **6**, 1283-1290.
20. I.-Y. Jeon, M. Choi, H.-J. Choi, S.-M. Jung, M.-J. Kim, J.-M. Seo, S.-Y. Bae, S. Yoo, G. Kim, H. Y. Jeong, N. Park and J.-B. Baek, *Nat. Commun.*, 2015, 6, 7123.
21. S. Azevedo, C. Chesman and J. R. Kaschny, *Eur. Phys. J. B*, 2010, **74**, 123-128.
22. T. W. Odom, *Aust. J. Chem.*, 2001, **54**, 601-604.
23. L. Guo, D. G. Morris, X. Liu, C. Vaslet, R. H. Hurt and A. B. Kane, *Chem. Mater.*, 2007, **19**, 3472-3478.
24. X. Liu, V. Gurel, D. Morris, D. W. Murray, A. Zhitkovich, A. B. Kane and R. H. Hurt, *Adv. Mater.*, 2007, **19**, 2790-2796.
25. C. E. Banks, A. Crossley, C. Salter, S. J. Wilkins and R. G. Compton, *Angew. Chem. Int. Ed.*, 2006, **45**, 2533-2537.
26. B. Šljukić, C. E. Banks and R. G. Compton, *Nano Lett.*, 2006, **6**, 1556-1558.
27. C. Batchelor-McAuley, G. G. Wildgoose, R. G. Compton, L. Shao and M. L. H. Green, *Sens. Actuators B Chem*, 2008, **132**, 356-360.
28. X. Dai, G. G. Wildgoose and R. G. Compton, *Analyst*, 2006, **131**, 901-906.
29. X. Tian, S. Zhou, Z. Zhang, X. He, M. Yu and D. Lin, *Environ. Sci. Technol.*, 2010, **44**, 8144-8149.
30. X. Liu, L. Guo, D. Morris, A. B. Kane and R. H. Hurt, *Carbon*, 2008, **46**, 489-500.
31. S. Koyama, Y. A. Kim, T. Hayashi, K. Takeuchi, C. Fujii, N. Kuroiwa, H. Koyama, T. Tsukahara and M. Endo, *Carbon*, 2009, **47**, 1365-1372.
32. L. Wang, C. K. Chua, B. Khezri, R. D. Webster and M. Pumera, *Electrochem. Commun.*, 2016, **62**, 17-20.
33. Y. Dong, J. Li, L. Shi and Z. Guo, *ACS Appl. Mater. Interfaces*, 2015, **7**, 15403-15413.
34. A. Ambrosi, S. Y. Chee, B. Khezri, R. D. Webster, Z. Sofer and M. Pumera, *Angew. Chem. Int. Ed.*, 2012, **51**, 500-503.
35. A. Ambrosi, C. K. Chua, B. Khezri, Z. Sofer, R. D. Webster and M. Pumera, *Proc. Natl. Acad. Sci. U. S. A.*, 2012, **109**, 12899-12904.
36. C. H. A. Wong, Z. Sofer, M. Kubešová, J. Kučera, S. Matějková and M. Pumera, *Proc. Natl. Acad. Sci. U. S. A.*, 2014, **111**, 13774-13779.
37. C. K. Chua, A. Ambrosi, Z. Sofer, A. Mackova, V. Havranek, I. Tomandl and M. Pumera, *Chem. Eur. J.*, 2014, **20**, 15760-15767.
38. A. Ambrosi and M. Pumera, *Nanoscale*, 2014, **6**, 472-476.
39. G. Lupina, J. Kitzmann, I. Costina, M. Lukosius, C. Wenger, A. Wolff, S. Vaziri, M. Ostling, I. Pasternak, A. Krajewska, W. Strupinski, S. Kataria, A. Gahoi, M. C. Lemme, G. Ruhl, G. Zoth, O. Luxenhofer and W. Mehr, *ACS Nano*, 2015, **9**, 4776-4785.
40. C. H. A. Wong and M. Pumera, *J. Phys. Chem. C*, 2016, **120**, 4682-4690.
41. C. K. Chua and M. Pumera, *Chem. Eur. J.*, 2015, **21**, 12550–12562
42. J. S. Bunch, A. M. van der Zande, S. S. Verbridge, I. W. Frank, D. M. Tanenbaum, J. M. Parpia, H. G. Craighead and P. L. McEuen, *Science*, 2007, **315**, 490-493.
43. Z. Ni, Y. Wang, T. Yu and Z. Shen, *Nano Research*, 2008, **1**, 273-291.
44. C. H. A. Wong, Z. Sofer, M. Kubesova, J. Kucera, S. Matejkova and M. Pumera, *Proc. Natl. Acad. Sci. U. S. A.*, 2014, **111**, 13774-13779.
45. E. J. E. Stuart and M. Pumera, *J. Phys. Chem. C*, 2010, **114**, 21296-21298.
46. T. J. Davies, M. E. Hyde and R. G. Compton, *Angew. Chem. Int. Ed.*, 2005, **44**, 5121-5126.
47. *US Pat.*, US2914383 A, 1959.
48. Wang, H. Shan, R. H. Hauge, M. Pasquali and R. E. Smalley, *J. Phys. Chem. B*, 2007, **111**, 1249-1252.
49. E. Dujardin, T. W. Ebbesen, A. Krishnan and M. M. J. Treacy, *Adv. Mater.*, 1998, **10**, 611-613.
50. A. G. Rinzler, J. Liu, H. Dai, P. Nikolaev, C. B. Huffman, F. J. Rodríguez-Macías, P. J. Boul, A. H. Lu, D. Heymann, D. T. Colbert, R. S. Lee, J. E. Fischer, A. M. Rao, P. C. Eklund and R. E. Smalley, *Appl. Phys. A*, 1998, **67**, 29-37.
51. R. R. Prajapati, T. G. Srinivasan, V. Chandramouli and S. S. Bhagwat, *Desalination and Water Treatment*, 2014, **52**, 490-497.